

# THE KOLMOGOROV-AVRAMI TYPE MODELS OF CRYSTAL GROWTH IN LIMITED VOLUMES

Tomoyuki NAGAYA, Hiroshi ORIHARA and Yoshihiro ISHIBASHI

*Synthetic Crystal Research Laboratory*

(Received October 28, 1993)

## Abstract

The formulas previously derived for finite systems on the basis of the Kolmogorov-Avrami model are applied to the growth on the periphery of circles and on the surface of spheres, which are of a finite size but without boundaries. The inward growth with nuclei existing only on the periphery and the surface is also studied. The position dependence of the fractional transformed volumes is explicitly shown. Results are discussed in relation to ferroelectric polarization reversals.

## Keywords

Kolmogorov-Avrami model, crystal growth, finite systems, ferroelectric polarization reversal

## §1. Introduction

In a previous paper the authors have derived the formulas of the time dependence of the transformed volume (the reversed domain in the case of ferroelectric polarization reversals) in terms of the Kolmogorov-Avrami model, where the finiteness of the sample size is explicitly taken into account.<sup>1)</sup> On the basis of the obtained formulas, several concrete cases of practical importance have been studied.<sup>2),3)</sup> Ferroelectric switching is one of such examples. Analyses of the switching processes in ferroelectric thin films are important from the viewpoint of their applications to non-volatile memory.<sup>4)</sup> In them the consideration of finiteness seems now of special necessity,<sup>5),6)</sup> because down-sizing of the memory cells has been remarkably advanced recently.

The purpose of the present paper is to apply the mathematical method developed

previously for treating finite systems to study another kind of finite systems, which are finite but without boundaries (except for the periphery or the surface itself). In §2 various cases are considered and numerical results are presented, and in §3 results will be discussed, in particular, in relation to ferroelectric polarization reversals.

## §2. Models

In this section, the formulas for the growth in finite systems are derived. As finite systems we consider a circle and a sphere of the radius  $R$ . Nuclei are assumed to exist only on the periphery of the circle and the surface of the sphere. The velocity of the movement of the boundary between the transformed and non-transformed regions is denoted as  $v$ .

### A. A circle

[Aa] On-periphery growth.

(Aa-1) Category I, random nucleation.

Take a point P (Fig.1). The probability that P is included in the transformed region,  $Q(t)$ , is written as

$$Q(t) = 1 - e^{-J \int_0^t S(t, \tau) d\tau}, \quad (1)$$

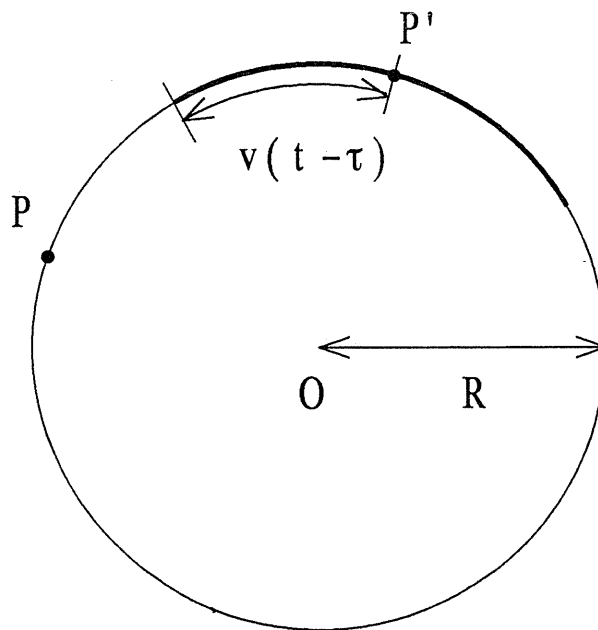


Fig. 1 A point P on the periphery of a circle. A domain starts at P'.

where  $J$  is the nucleation probability, and  $S(t, \tau)$  is the length at  $t$  covered by the transformed region starting from the nucleus born at  $t = \tau$ , i. e.,

$$S = \begin{cases} 2v(t - \tau), & \text{for } v(t - \tau) < \pi R, \\ 2\pi R, & \text{for } \pi R \leq v(t - \tau). \end{cases} \quad (2)$$

Therefore,

$$Q(t) = \begin{cases} 1 - e^{-Jvt^2}, & \text{for } 0 \leq t < \frac{\pi R}{v}, \\ 1 - e^{-J[2\pi Rt - \frac{\pi^2 R^2}{v}]}, & \text{for } \frac{\pi R}{v} \leq t. \end{cases} \quad (3)$$

These are shown in Fig. 2, where

$$t_J = \frac{1}{\sqrt{Jv}}, \quad l = R/\sqrt{v/J} \quad (4)$$

are used.

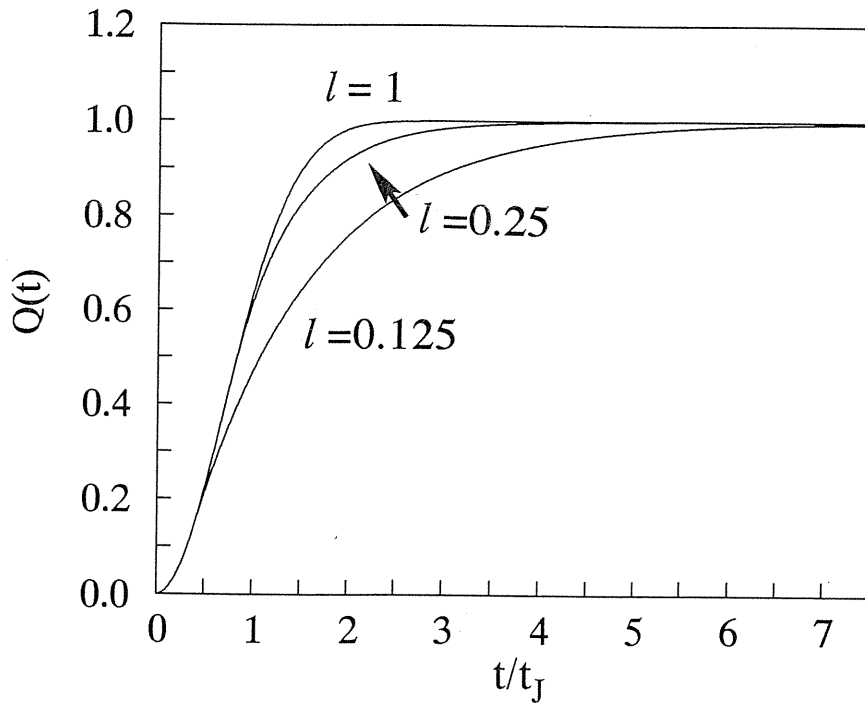


Fig. 2  $Q(t)$  for the on-periphery growth for various  $l$ . Category I.  $v = 1, J = 1$ .

(Aa-II) Category II, latent nuclei.

In this case, nucleation can be considered to take place only at  $\tau = 0$  for a short interval  $\Delta\tau$  with keeping  $J\Delta\tau = N$ . Thus,  $Q(t)$  are easily obtained as

$$Q(t) = \begin{cases} 1 - e^{-2\nu Nt}, & 0 \leq t < \frac{\pi R}{\nu}, \\ 1 - e^{-2\pi NR}, & \frac{\pi R}{\nu} \leq t. \end{cases} \quad (5)$$

These are shown in Fig. 3, where

$$t_N = \frac{1}{N\nu}, \quad l = NR \quad (6)$$

are used. It should be noted that at  $t = \pi R/\nu$  all curves show a break.

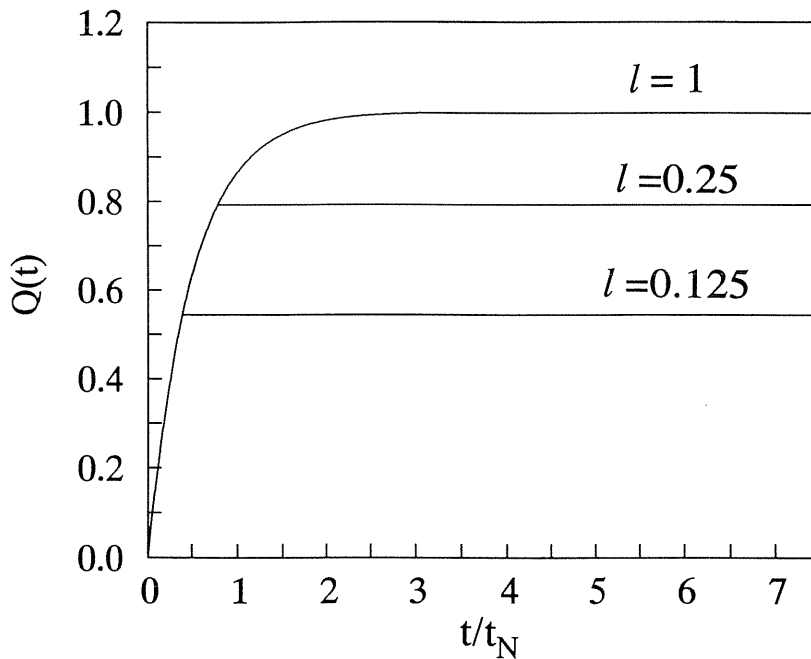


Fig. 3  $Q(t)$  for the on-periphery growth for various  $l$ . Category II.  
 $\nu = 1, N = 1$ .

[Ab] Inward growth.

(Ab-I) Category I, random nucleation.

Let us consider the case where nuclei exist on the periphery and the transformed regions

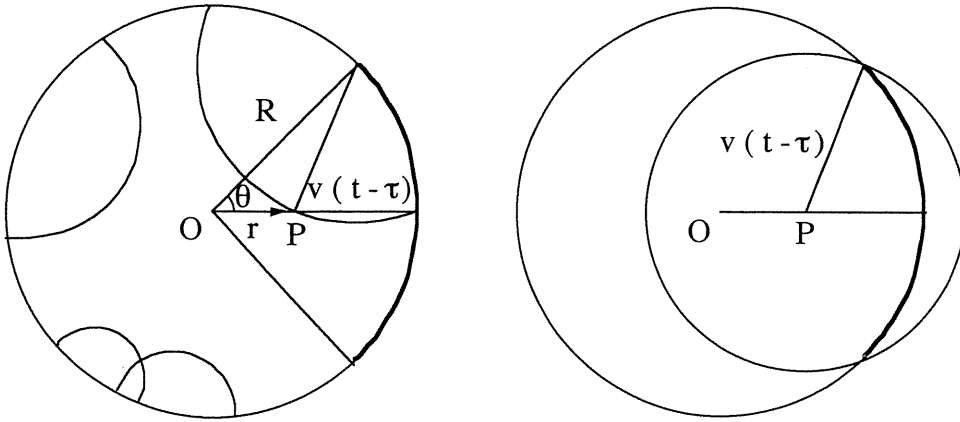


Fig. 4 Inward growth.

penetrate into inside (Fig. 4). Let us take a point P in the circle at a distance  $r$  from the center.

If no nucleation takes place on the arc (a part of periphery) which is included in a circle with the radius  $v(t - \tau)$  in the time interval  $\Delta \tau$  at various  $\tau$ , P is not included in the transformed region. Therefore,

$$q_r(t) = 1 - e^{-\int_0^t S(t, \tau) d\tau} \tag{7}$$

where  $S(t, \tau)$  is given as

$$S(t, \tau) = \begin{cases} 0, & \text{for } v(t - \tau) < R - r, \\ 2R\theta, & \text{for } R - r \leq v(t - \tau) < R + r, \\ 2R\pi, & \text{for } R + r \leq v(t - \tau), \end{cases} \tag{8}$$

where it is seen from Fig. 4 that  $\theta$  is given by

$$v^2(t - \tau)^2 = R^2 + r^2 - 2Rr \cos \theta. \tag{9}$$

Obviously, for  $0 \leq t < (R - r)/v$

$$q_r(t) = 0. \tag{10}$$

For other  $t$ ,  $q_r(t)$  can be obtained numerically. The results are shown Fig. 5. It should be noted that  $q_r(t)$  curves show crossing, though it is not clear from Fig. 5(a) for the case of large  $R$ . The crossing is much clearly seen for cases of smaller  $R$ .

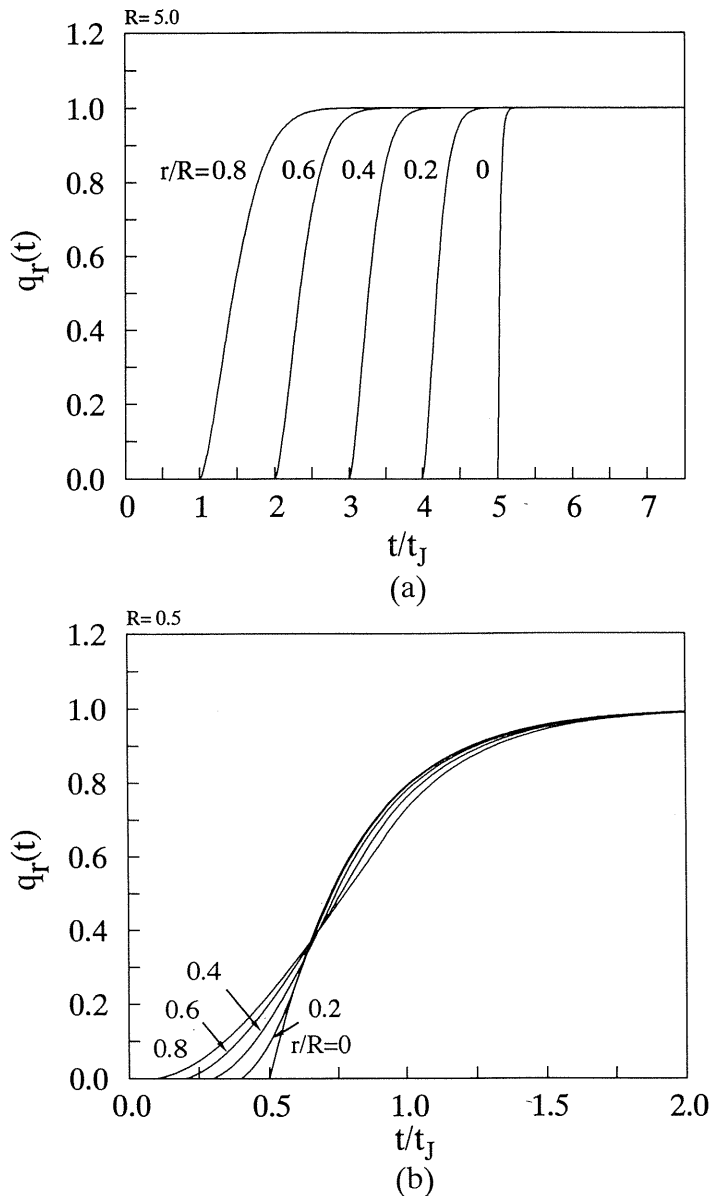


Fig. 5  $q_r(t)$  for the inward growth for various  $r$ . Category I.  
 (a)  $\nu = 1, J = 1, R = 5$ , (b)  $\nu = 1, J = 1, R = 0.5$ .

In Fig. 6 the position ( $d$ ) dependences of  $q_r(t)$  at the given  $t$  are shown for various cross sections cut at the distance  $r_0$  from the center (Fig. 7). They are very different depending on  $R$  and  $r_0$ , as can be seen by comparing Figs. 6(a)–(c) and Figs. 6(d)–(f). The difference obviously reflects the crossing of the  $q_r(t)$  curves shown in Fig. 5 (see Fig. 7 with respect to the relationship among  $d$ ,  $r_0$  and  $r$ ).

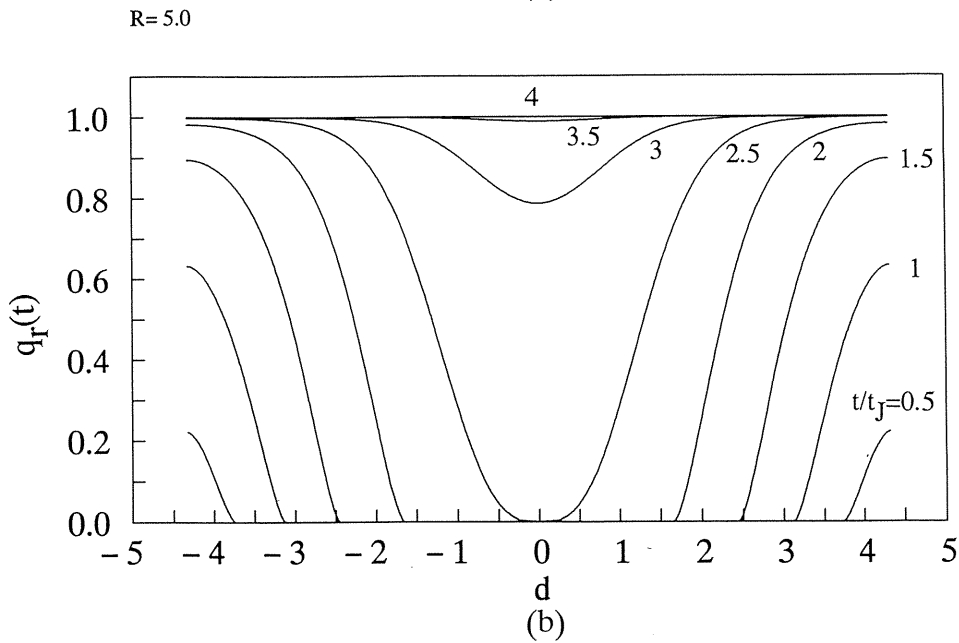
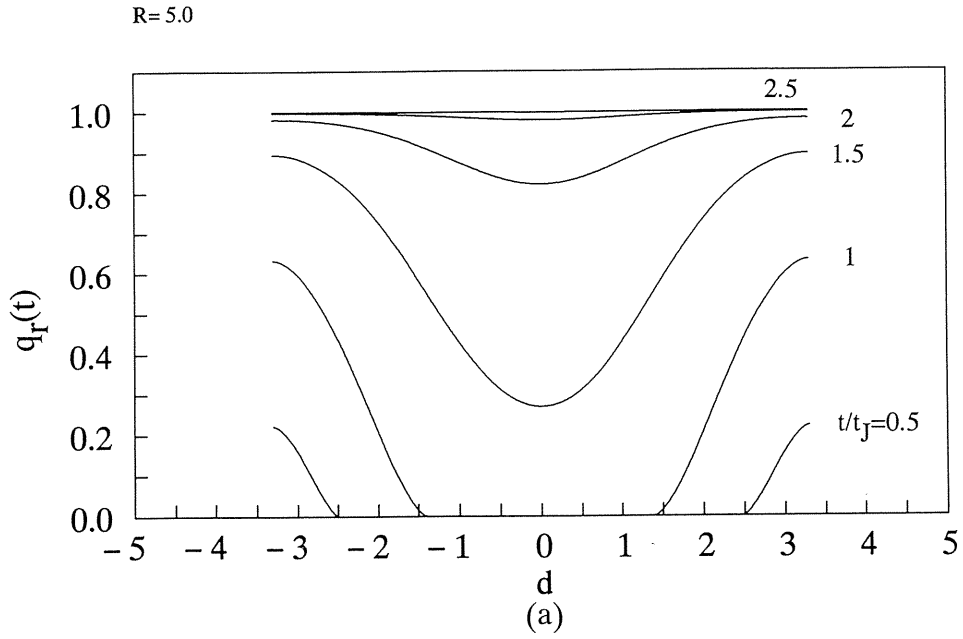


Fig. 6 The  $q_r(t)$  for the inward growth for various  $t$ . Category I.  
 For (a)–(c),  $\nu = 1$ ,  $J = 1$ ,  $R = 5$ , and (a)  $r_0 = 3.75$ , (b)  $r_0 = 2.5$  and (c)  $r_0 = 0$ .  
 For (d)–(f),  $\nu = 1$ ,  $J = 1$ ,  $R = 0.5$ , and (d)  $r_0 = 0.375$  (e)  $r_0 = 0.25$ , and (f)  $r_0 = 0$ . With respect to  $r_0$ , see Fig. 7.

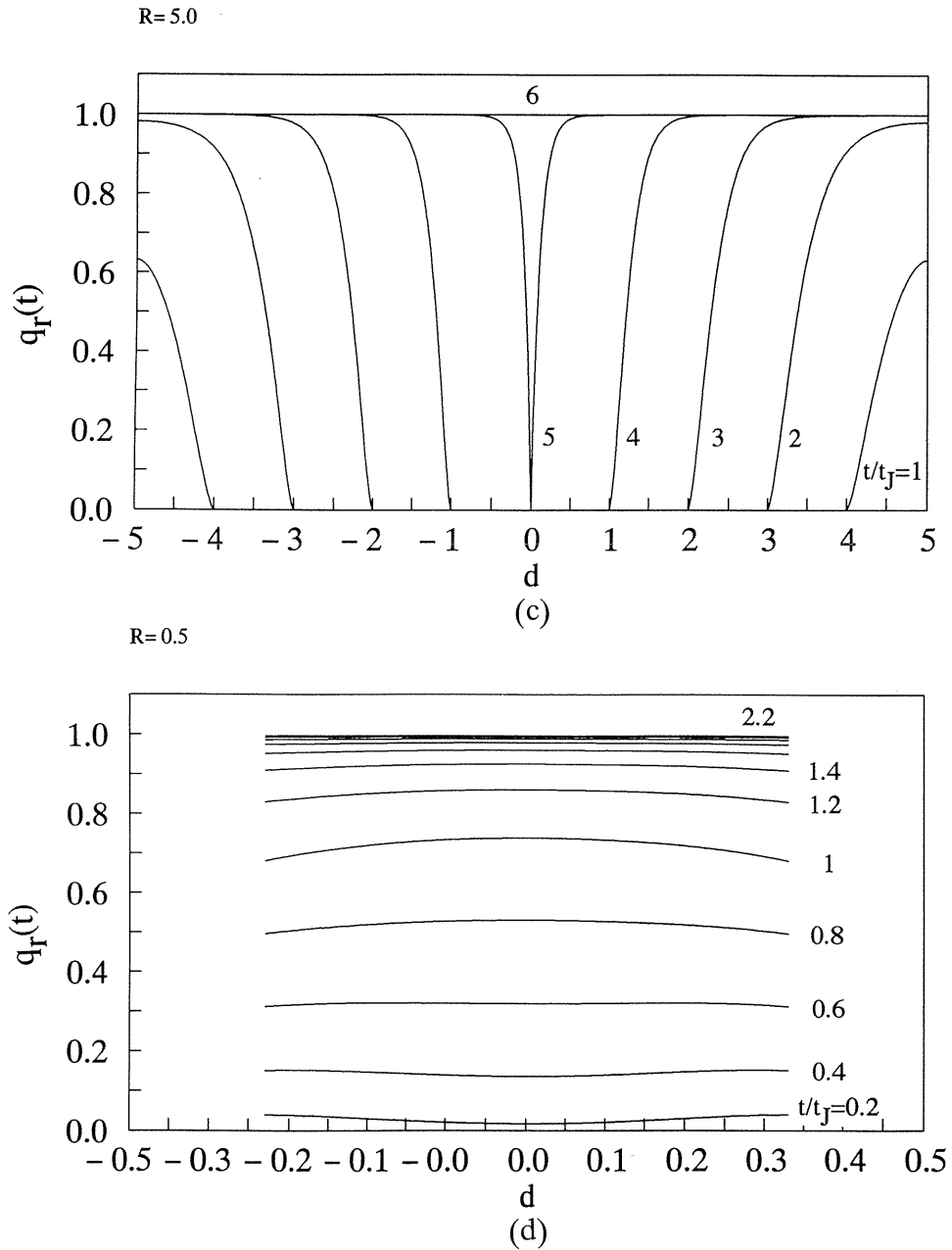


Fig. 6 The  $q_r(t)$  for the inward growth for various  $t$ . Category I.  
 For (a)–(c),  $\nu = 1$ ,  $J = 1$ ,  $R = 5$ , and (a)  $r_0 = 3.75$ , (b)  $r_0 = 2.5$  and (c)  $r_0 = 0$ .  
 For (d)–(f),  $\nu = 1$ ,  $J = 1$ ,  $R = 0.5$ , and (d)  $r_0 = 0.375$  (e)  $r_0 = 0.25$ , and (f)  $r_0 = 0$ . With respect to  $r_0$ , see Fig. 7.



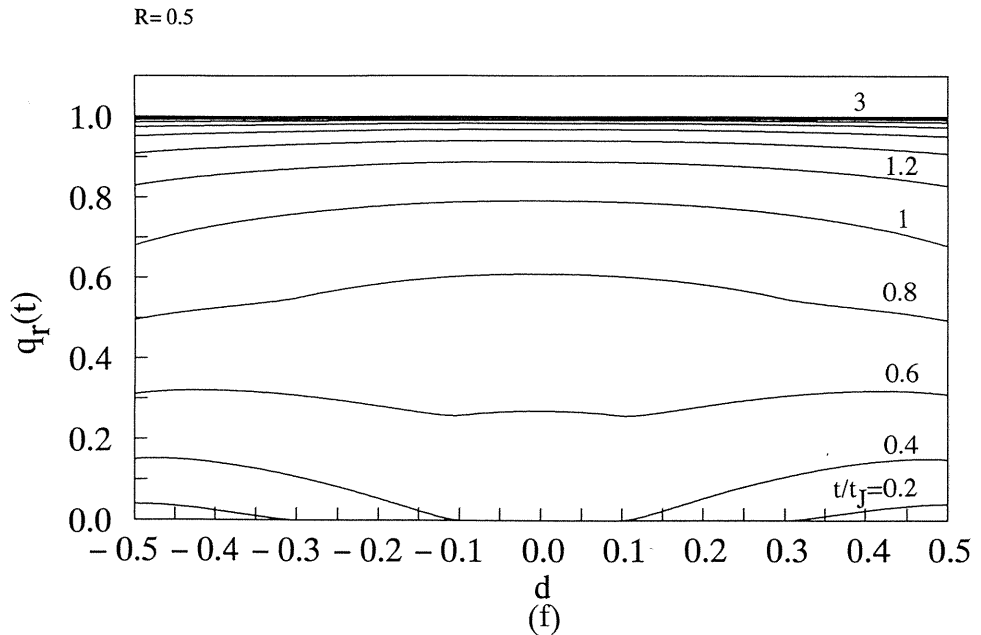
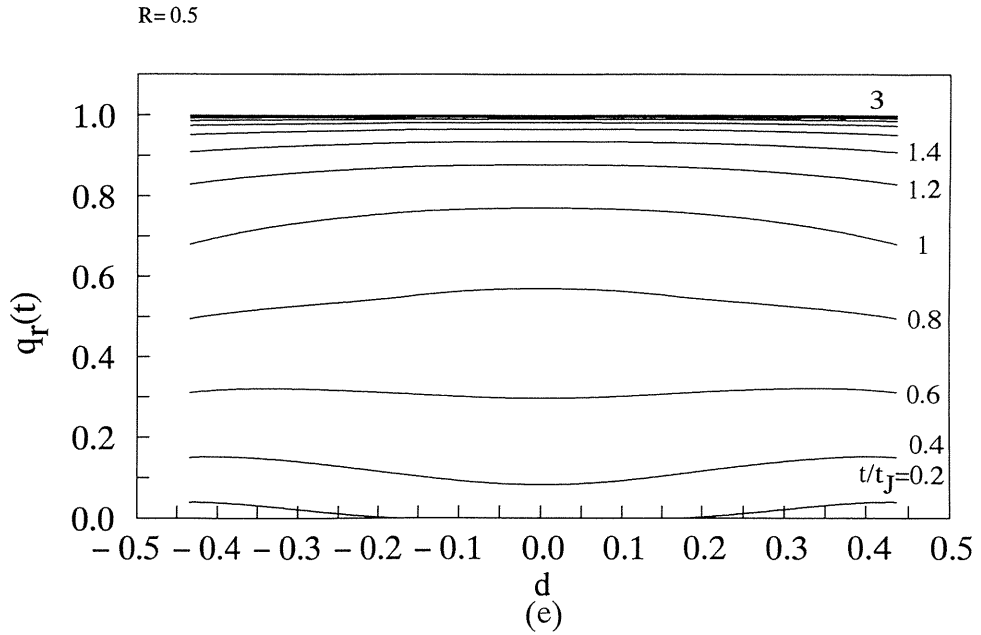
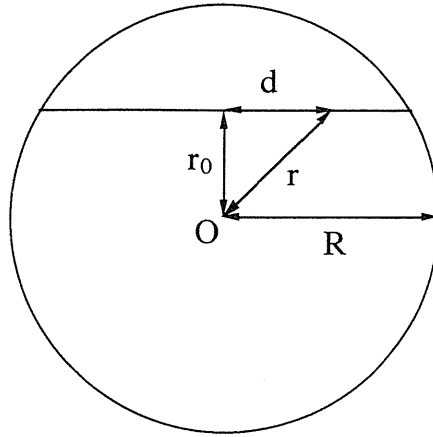


Fig. 6 The  $q_r(t)$  for the inward growth for various  $t$ . Category I.

For (a)–(c),  $\nu = 1$ ,  $J = 1$ ,  $R = 5$ , and (a)  $r_0 = 3.75$ , (b)  $r_0 = 2.5$  and (c)  $r_0 = 0$ .

For (d)–(f),  $\nu = 1$ ,  $J = 1$ ,  $R = 0.5$ , and (d)  $r_0 = 0.375$  (e)  $r_0 = 0.25$ , and (f)  $r_0 = 0$ . With respect to  $r_0$ , see Fig. 7.

Fig. 7 Notations;  $r_0$ ,  $d$  and  $r$ .

(Ab-II) Category II, latent nuclei.

In this case, P is included at time  $t$  in the transformed region if more than one latent nucleus exist on the arc included in the circle with the radius  $\nu t$  centered at P, while P is not included for otherwise. Therefore, the probability P is included in the transformed region is given as

$$q_r(t) = 1(1 - p) + 0 \cdot p, \quad (11)$$

where  $p$  is the probability that no latent nucleus exists in the concerned area, i.e.,

$$p = e^{-2R\theta}, \quad (12)$$

where

$$\theta = \begin{cases} 0, & \text{for } 0 \leq t < \frac{R-r}{\nu}, \\ \theta_0, & \text{for } \frac{R-r}{\nu} \leq t < \frac{R+r}{\nu}, \\ \pi, & \text{for } \frac{R+r}{\nu} \leq t, \end{cases} \quad (13)$$

$\theta_0$  being given as

$$\nu^2 t^2 = R^2 + r^2 - 2Rr \cos \theta_0. \quad (14)$$

The results are shown in Fig. 8. The position dependences of  $q_r(t)$  at the given  $t$  for various cross sections (see Fig. 7) are shown in Fig. 9. Same comments as given in (Ab-I) apply here, too.

The average fraction of the transformed region is obtained as

$$Q(t) = \frac{2}{R^2} \int_0^R r q_r(t) dr, \tag{15}$$

and  $Q(t)$  and  $dQ(t)/dt$  are shown in Fig. 10 for both of categories I and II.

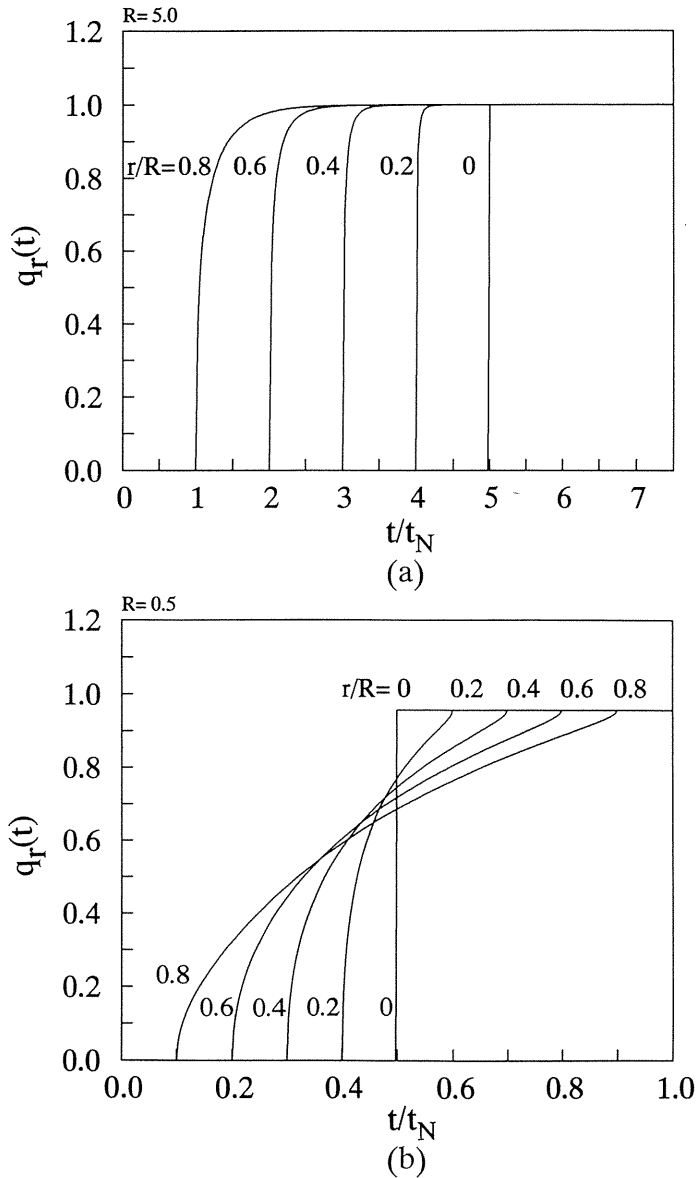


Fig. 8  $q_r(t)$  for the inward growth for various  $r$ . Category II. (a)  $\nu = 1, N = 1, R = 5$ . (b)  $\nu = 1, N = 1, R = 0.5$ .

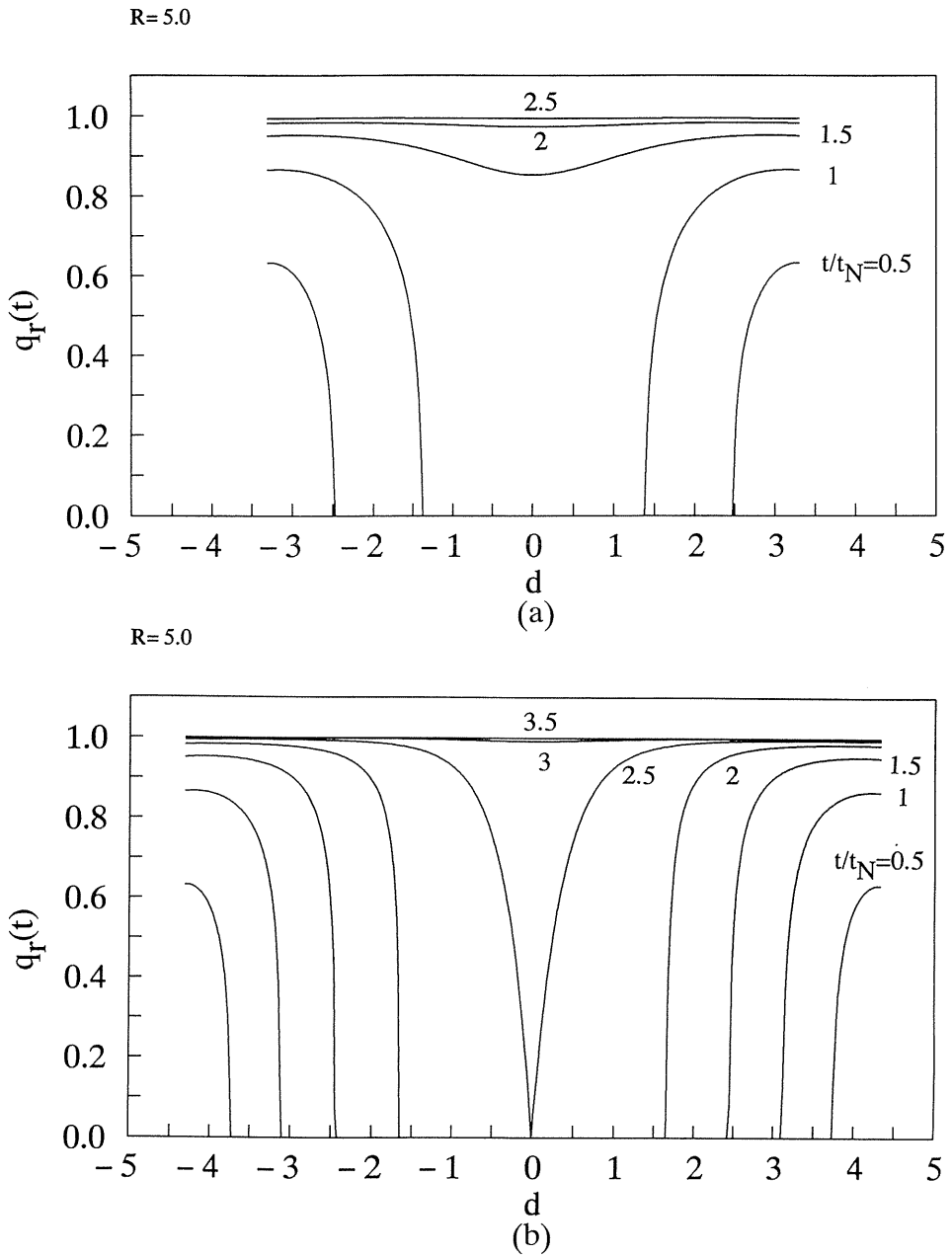


Fig. 9  $q(r, t)$  for the inward growth for various  $t$ . Category II.  
 For (a)–(c),  $\nu = 1$ ,  $N = 1$ ,  $R = 5$ , and (a)  $r_0 = 3.75$ , (b)  $r_0 = 2.5$  and (c)  $r_0 = 0$ .  
 For (d)–(f),  $\nu = 1$ ,  $R = 0.5$ , and (d)  $r_0 = 0.375$ , (e)  $r_0 = 0.25$  and (f)  $r_0 = 0$ .

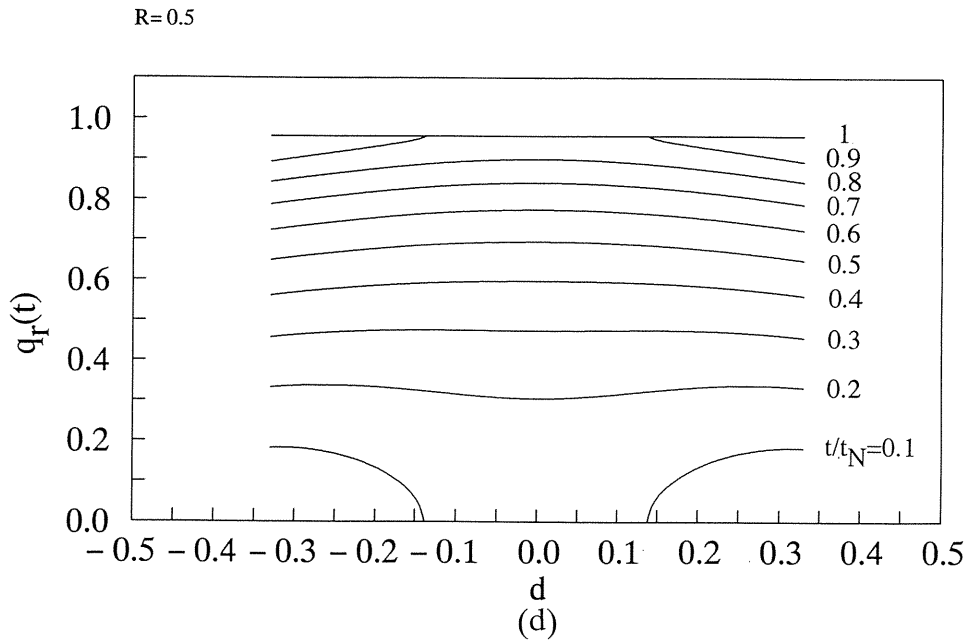
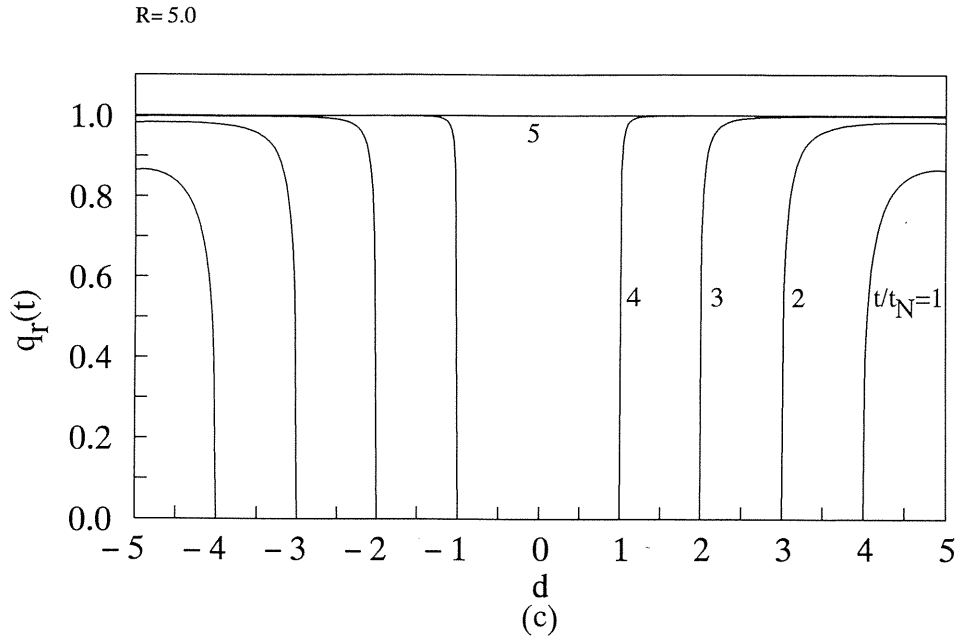


Fig. 9  $q(r, t)$  for the inward growth for various  $t$ . Category II.  
 For (a)–(c),  $\nu = 1$ ,  $N = 1$ ,  $R = 5$ , and (a)  $r_0 = 3.75$ , (b)  $r_0 = 2.5$  and (c)  $r_0 = 0$ .  
 For (d)–(f),  $\nu = 1$ ,  $R = 0.5$ , and (d)  $r_0 = 0.375$ , (e)  $r_0 = 0.25$  and (f)  $r_0 = 0$ .

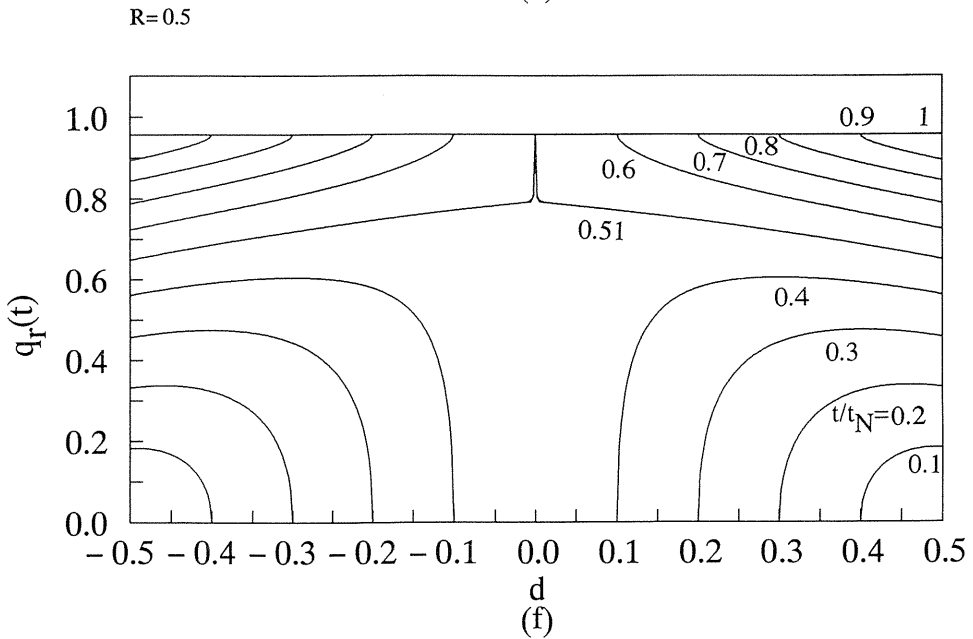
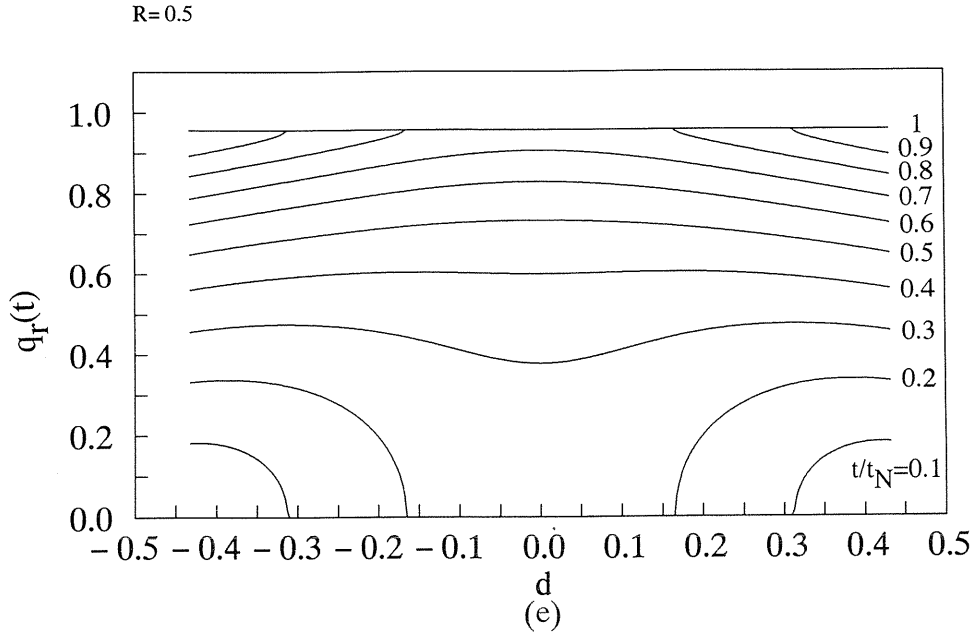


Fig. 9  $q(r, t)$  for the inward growth for various  $t$ . Category II.  
 For (a)–(c),  $\nu = 1$ ,  $N = 1$ ,  $R = 5$ , and (a)  $r_0 = 3.75$ , (b)  $r_0 = 2.5$  and (c)  $r_0 = 0$ .  
 For (d)–(f),  $\nu = 1$ ,  $R = 0.5$ , and (d)  $r_0 = 0.375$ , (e)  $r_0 = 0.25$  and (f)  $r_0 = 0$ .

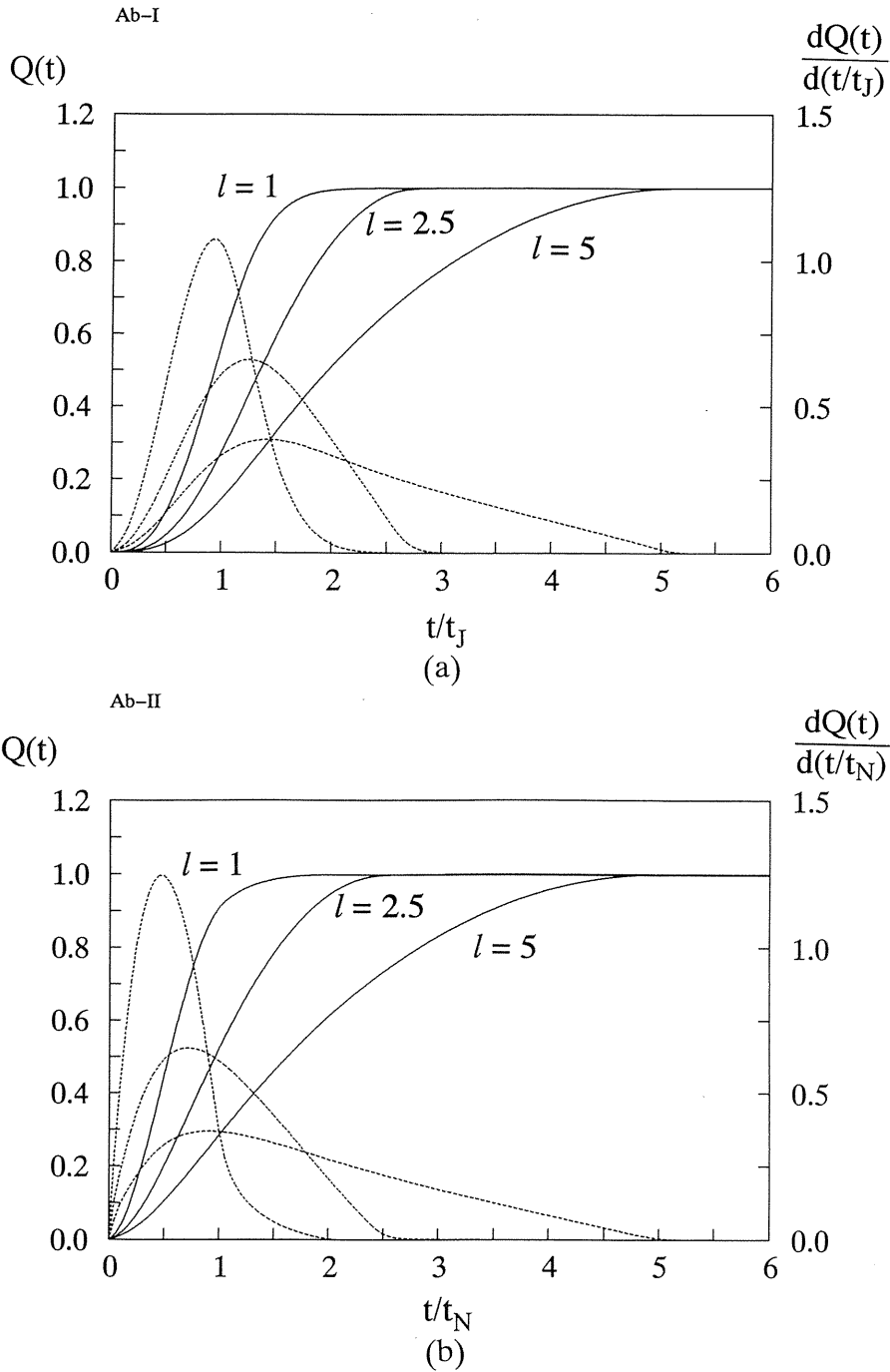


Fig. 10 The average fraction of the transformed region for a circle with (dashed lines) which corresponds to the switching currents due to polarization reversals. (a) Category I, and (b) category II.

B. A sphere

[Ba] On-surface growth.

(Ba-I) Category I, random nucleation.

Take a point P on the surface (Fig. 11). The probability that P is not included in the transformed region is given by eq. (1), where in the present case  $S(t, \tau)$  is given as

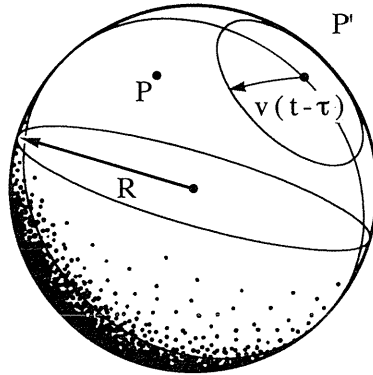


Fig. 11 A point P on the surface of a sphere. A domain starts at P'.

$$S(t, \tau) = \begin{cases} 2\pi R^2(1 - \cos\theta_0), & \text{for } 0 \leq t - \tau < \frac{\pi R}{v}, \\ 4\pi R^2, & \text{for } \frac{\pi R}{v} \leq t - \tau, \end{cases} \quad (16)$$

where  $\theta_0$  is given as

$$R\theta_0 = v(t - \tau).$$

Therefore,  $Q(t)$  is obtained as

$$Q(t) = \begin{cases} 1 - \exp\left[-2\pi J R^2 \left(t - \frac{R}{v} \sin \frac{vt}{R}\right)\right], & \text{for } 0 \leq t < \frac{\pi R}{v}, \\ 1 - \exp\left[-2\pi J R^2 \left(2t - \frac{\pi R}{v}\right)\right], & \text{for } \frac{\pi R}{v} \leq t. \end{cases} \quad (17)$$

There  $Q(t)$  are shown in Fig. 12, where the characteristic time and length

$$t_j = \left(\frac{1}{Jv^2}\right)^{1/3}, \quad l = R/(v/J)^{1/3} \quad (18)$$

are used.



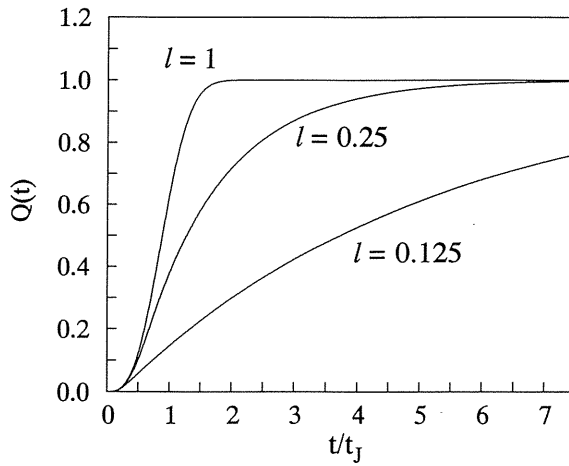


Fig. 12  $Q(t)$  for the on-surface growth for various  $l$ . Category I.  $\nu = 1, J = 1$ .

*(Ba-II) Category II, latent nuclei.*

The situation is simpler than in the case of the category I, and  $Q(t)$  is given as

$$Q(t) = \begin{cases} 1 - \exp\left[-2\pi NR^2\left(1 - \cos \frac{\nu t}{R}\right)\right], & 0 \leq t < \frac{\pi R}{\nu}, \\ 1 - \exp(-4\pi NR^2), & \frac{\pi R}{\nu} \leq t. \end{cases} \quad (19)$$

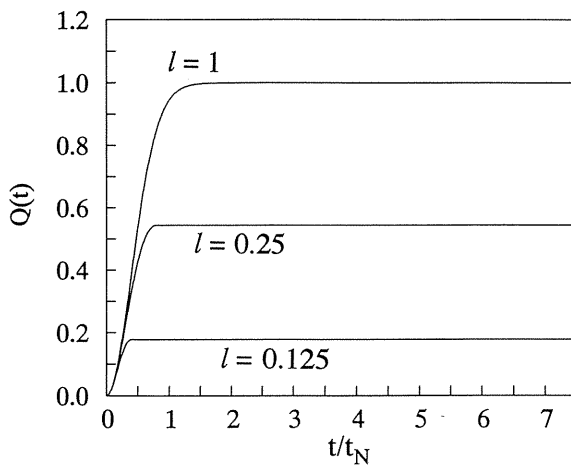


Fig. 13  $Q(t)$  for the on-surface growth for various  $l$ . Category II.  $\nu = 1, N = 1$ .

$Q(t)$  is shown in Fig. 13, where the characteristic time and length

$$t_N = \frac{1}{Nv}, \quad l = \sqrt{NR} \quad (20)$$

as used.

[Bb] Inward growth.

(Bb-I) Category I, random nucleation

Let us consider the case where nuclei exist only on the surface and the transformed regions penetrate into inside (Fig. 14). By the method adopted in [Ab],  $q_r(t)$  is obtained as

$$q_r(t) = 1 - e^{-J \int_0^t S(t, \tau) d\tau} \quad (21)$$

where  $S(t, \tau)$  is given as

$$S(t, \tau) = \begin{cases} 0, & 0 \leq v(t-\tau) < R-r, \\ 2\pi R^2(1 - \cos\theta_0), & R-r \leq v(t-\tau) < R+r \\ 4\pi R^2, & R+r \leq v(t-\tau), \end{cases} \quad (22)$$

$\theta_0$  being given by

$$v^2(t-\tau)^2 = R^2 + r^2 - 2Rr \cos\theta_0. \quad (23)$$

Since  $\cos\theta_0$  can be expressed with  $(t-\tau)^2$ , the integration in the argument in the exponential function in (21) can be easily performed, and the results are shown in Fig. 15.

The position dependences of  $q_r(t)$  for various cross sections are shown in Figs. 16(a)–(f). Similar comments as described in (Ab–I) apply here, too.

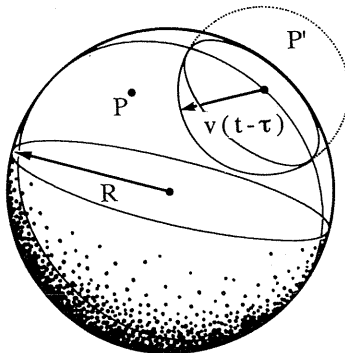


Fig. 14 Inward growth.

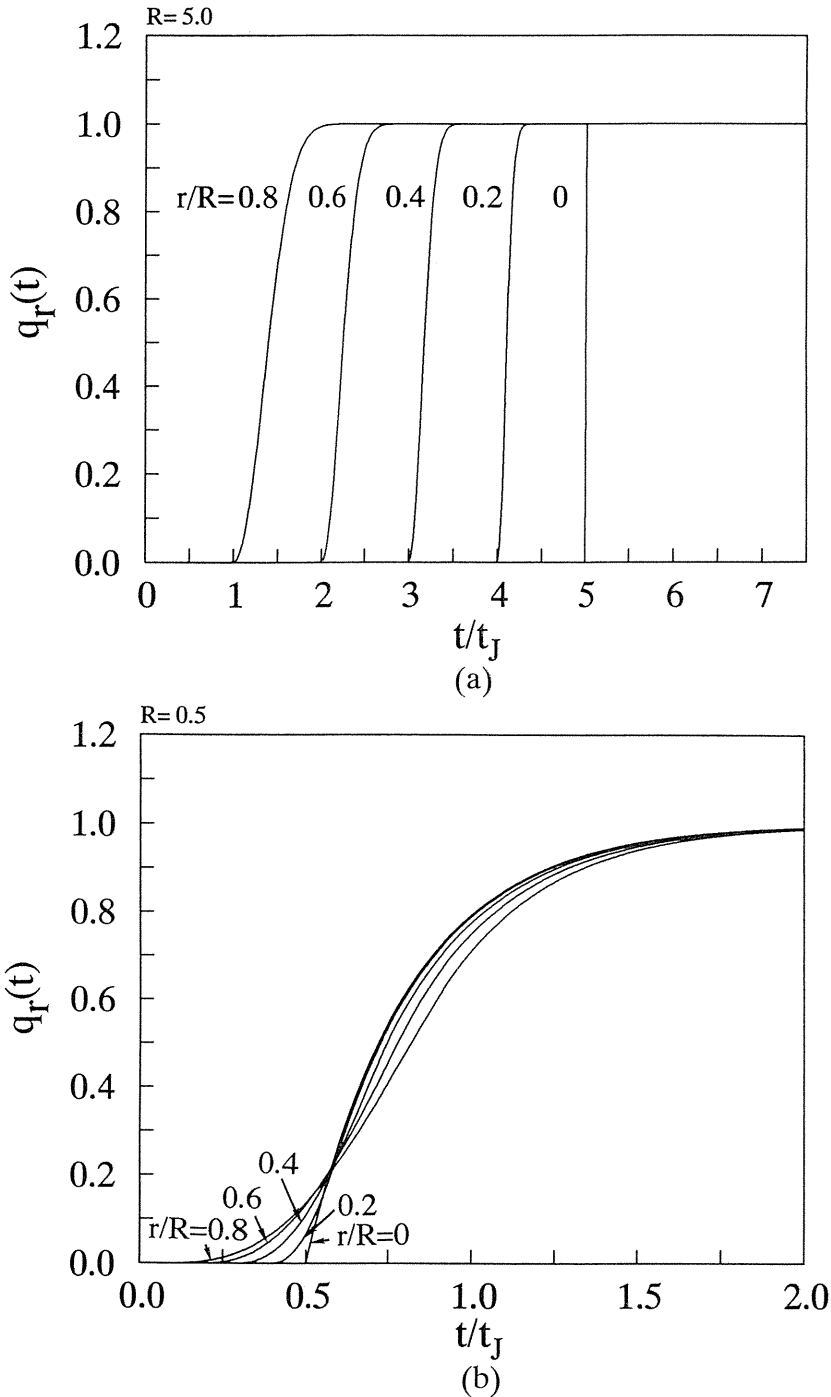


Fig. 15  $q_r(t)$  for the inward growth for various  $r$ . Category I.  
 (a)  $\nu = 1, J = 1, R = 5$ . (b)  $\nu = 1, J = 1, R = 0.5$ .

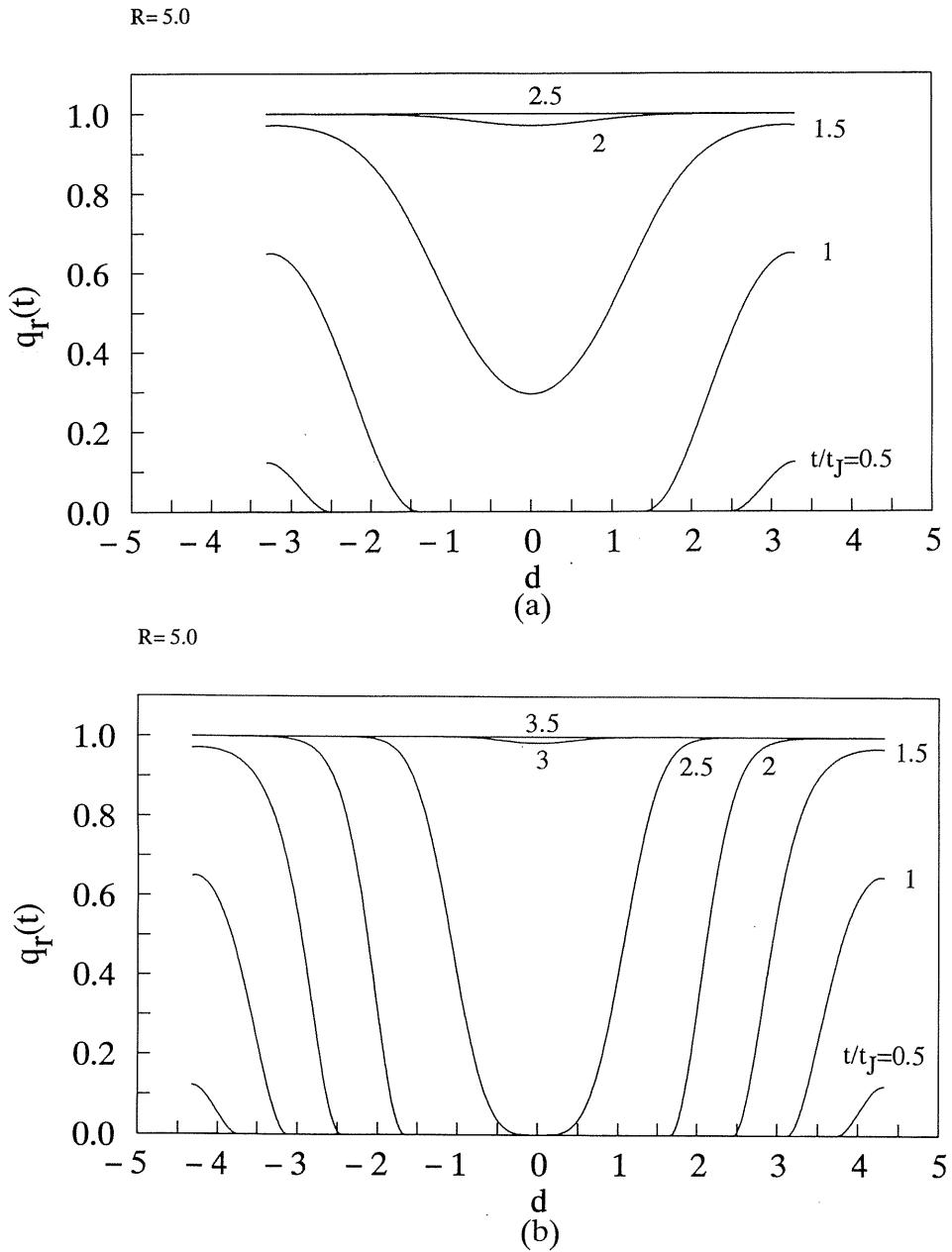


Fig. 16  $q_r(t)$  for the inward growth for various  $t$ . Category I.  
 For (a)–(c),  $\nu = 1$ ,  $N = 1$ ,  $R = 5$ , and (a)  $r_0 = 3.75$ , (b)  $r_0 = 2.5$  and (c)  $r_0 = 0$ . For  
 (d)–(f),  $\nu = 1$ ,  $J = 1$ ,  $R = 0.5$ , and (d)  $r_0 = 0.375$ , (e)  $r_0 = 0.25$  and (f)  $r_0 = 0$ .

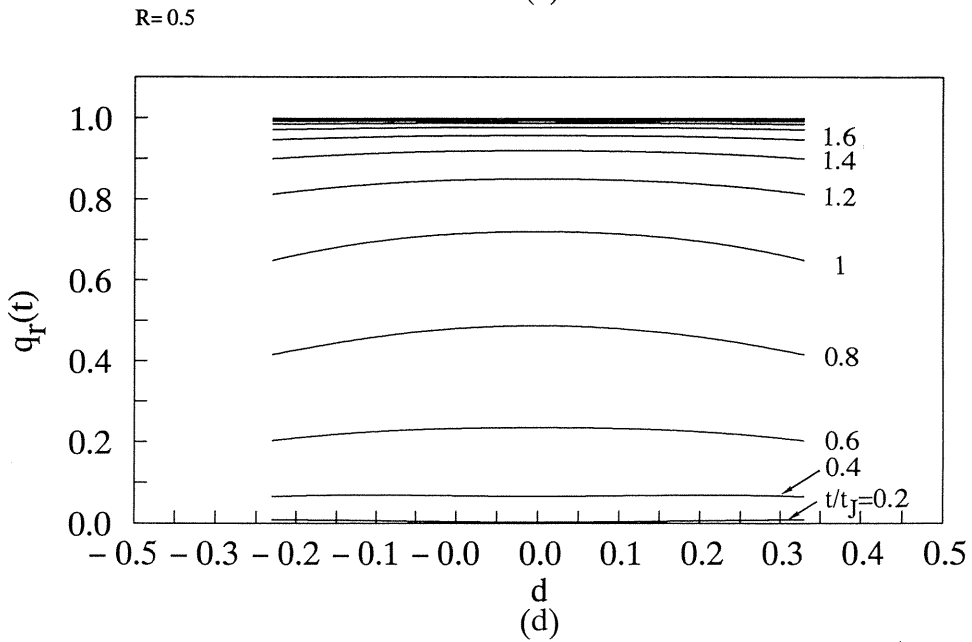
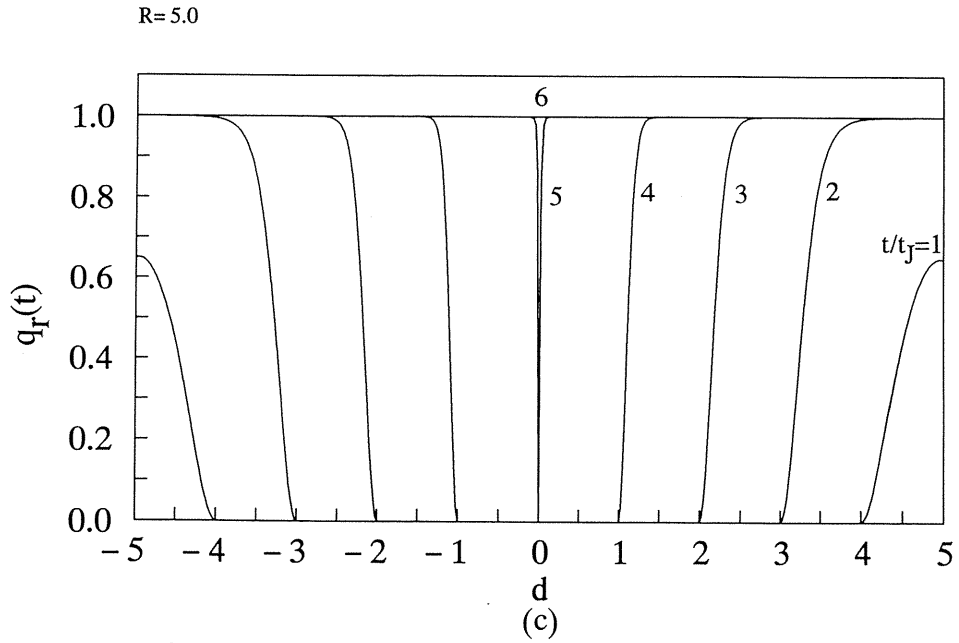


Fig. 16  $q_r(t)$  for the inward growth for various  $t$ . Category I.  
 For (a)–(c),  $\nu = 1$ ,  $N = 1$ ,  $R = 5$ , and (a)  $r_0 = 3.75$ , (b)  $r_0 = 2.5$  and (c)  $r_0 = 0$ . For  
 (d)–(f),  $\nu = 1$ ,  $J = 1$ ,  $R = 0.5$ , and (d)  $r_0 = 0.375$ , (e)  $r_0 = 0.25$  and (f)  $r_0 = 0$ .

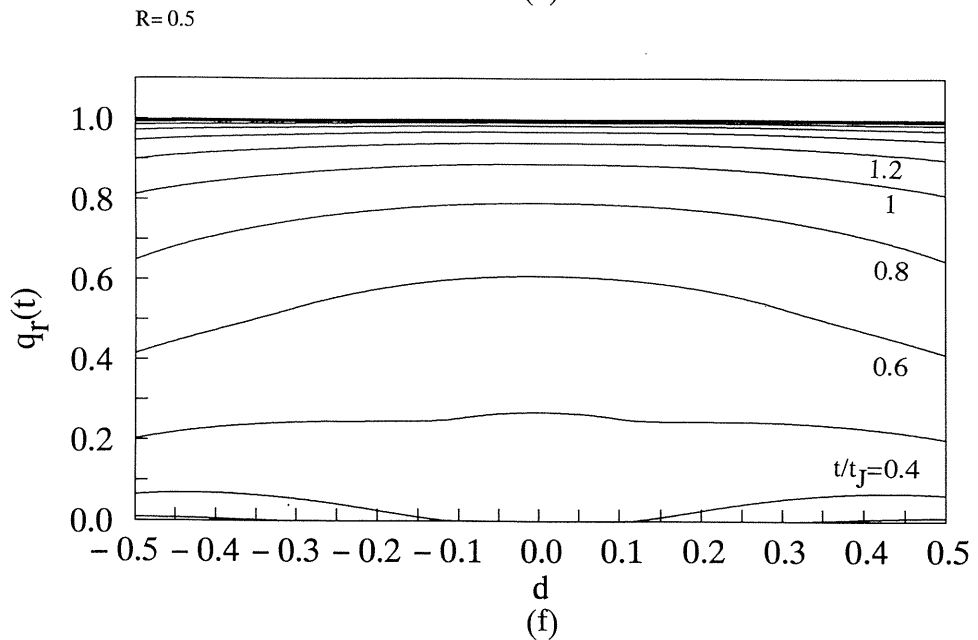
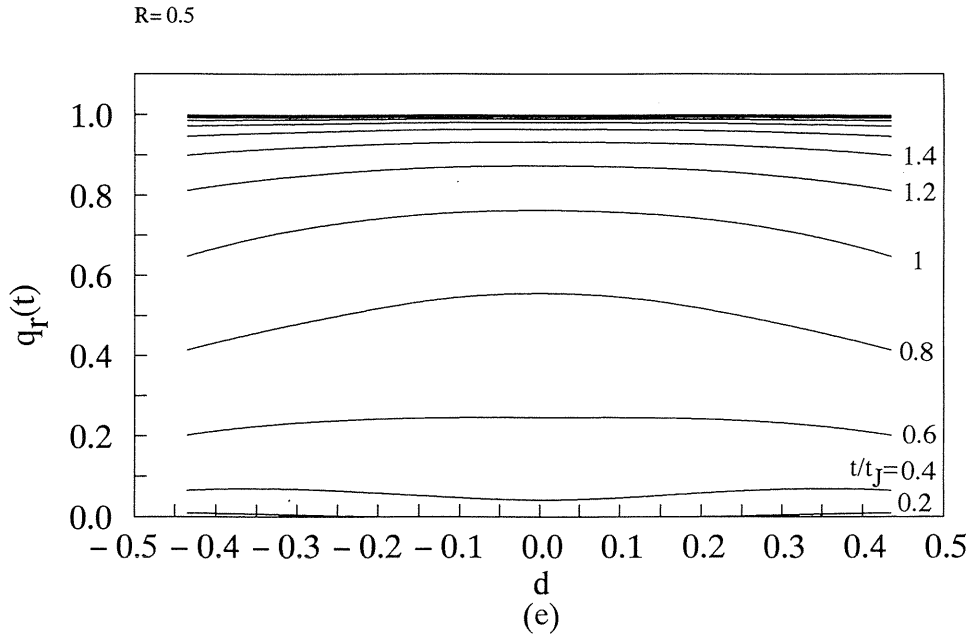


Fig. 16  $q_r(t)$  for the inward growth for various  $t$ . Category I.  
 For (a)–(c),  $\nu = 1$ ,  $N = 1$ ,  $R = 5$ , and (a)  $r_0 = 3.75$ , (b)  $r_0 = 2.5$  and (c)  $r_0 = 0$ . For  
 (d)–(f),  $\nu = 1$ ,  $J = 1$ ,  $R = 0.5$ , and (d)  $r_0 = 0.375$ , (e)  $r_0 = 0.25$  and (f)  $r_0 = 0$ .

(Bb-II) Category II, latent nuclei

By the same technique adopted in (Ab-II), we obtain

$$q_r(t) = \begin{cases} 0, & 0 \leq vt < R - r, \\ 1 - \exp[-2\pi R^2 N(1 - \cos\theta_0)], & R - r \leq vt < R + r, \\ 1 - \exp(-4\pi R^2 N), & R + r \leq vt, \end{cases} \quad (24)$$

where  $\theta_0$  is given as

$$v^2 t^2 = R^2 + r^2 - 2Rr \cos\theta_0. \quad (25)$$

These  $q_r(t)$  are shown in Fig. 17 and the  $q_r(t)$  at various cross sections are shown in Figs. 18(a)–(f). Similar comments as given in (Ab-I) apply here, too.

The average fraction of the transformed region for a sphere with the radius  $R$  is obtained as

$$Q(t) = \frac{3}{R^3} \int_0^R r^2 q_r(t) dr, \quad (26)$$

and  $Q(t)$  and  $dQ(t)/dt$  are shown in Fig. 19 for both of categories I and II.

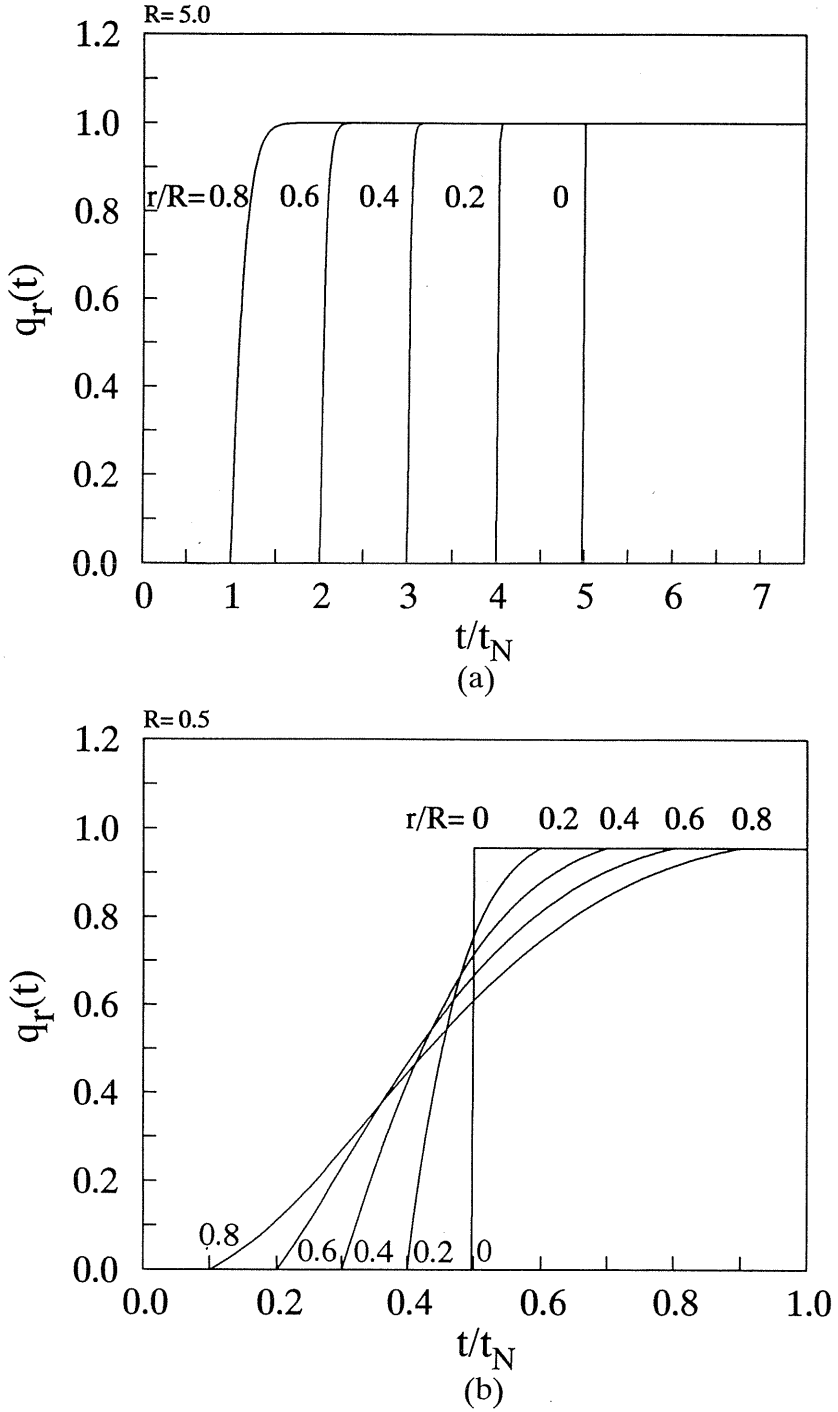


Fig. 17  $q_r(t)$  for the inward growth for various  $r$ . Category II.  
 (a)  $R = 5$ , (b)  $R = 0.5$ .



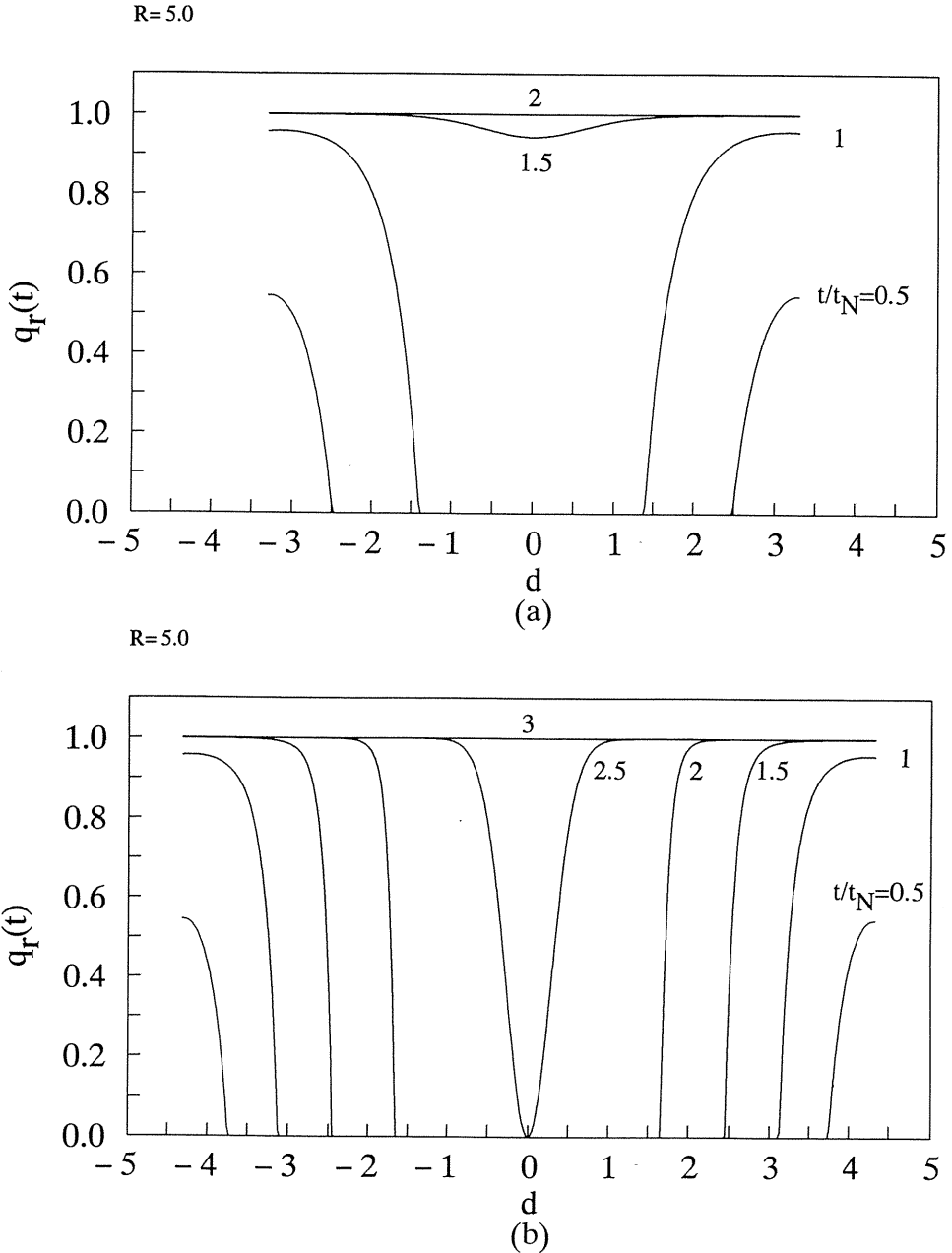


Fig. 18  $q_r(t)$  for the inward growth for various  $t$ . Category II.

For (a)–(c),  $\nu = 1$ ,  $J = 1$ ,  $R = 5$ , and (a)  $r_0 = 3.75$ , (b)  $r_0 = 2.5$  and (c)  $r_0$ . For (d)–(f),  $\nu = 1$ ,  $J = 1$ ,  $R = 0.5$ , and (d)  $r_0 = 0.375$ , (e)  $r_0 = 0.25$  and (f)  $r_0 = 0$ .

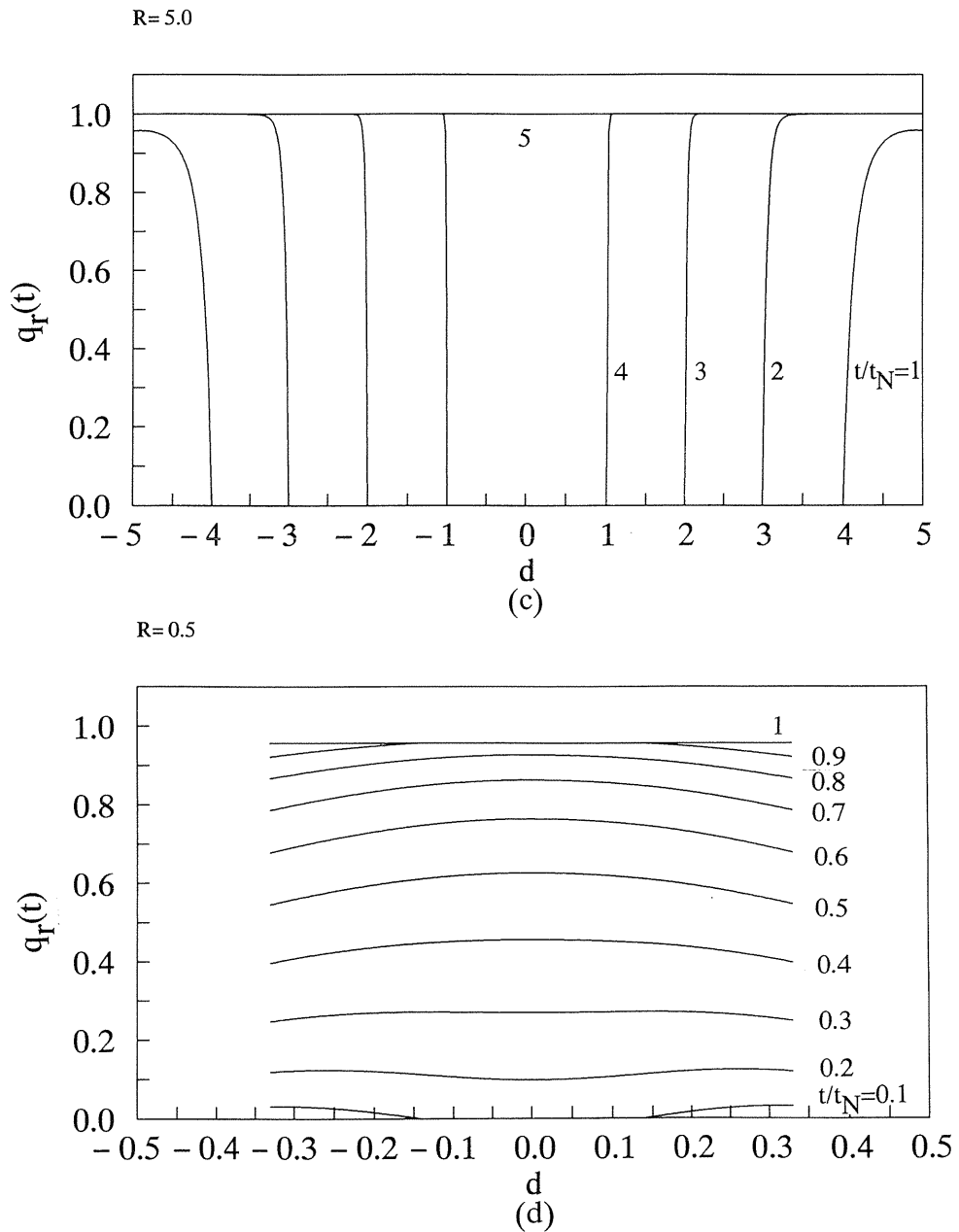


Fig. 18  $q_r(t)$  for the inward growth for various  $t$ . Category II.

For (a)–(c),  $\nu = 1$ ,  $J = 1$ ,  $R = 5$ , and (a)  $r_0 = 3.75$ , (b)  $r_0 = 2.5$  and (c)  $r_0$ . For (d)–(f),  $\nu = 1$ ,  $J = 1$ ,  $R = 0.5$ , and (d)  $r_0 = 0.375$ , (e)  $r_0 = 0.25$  and (f)  $r_0 = 0$ .

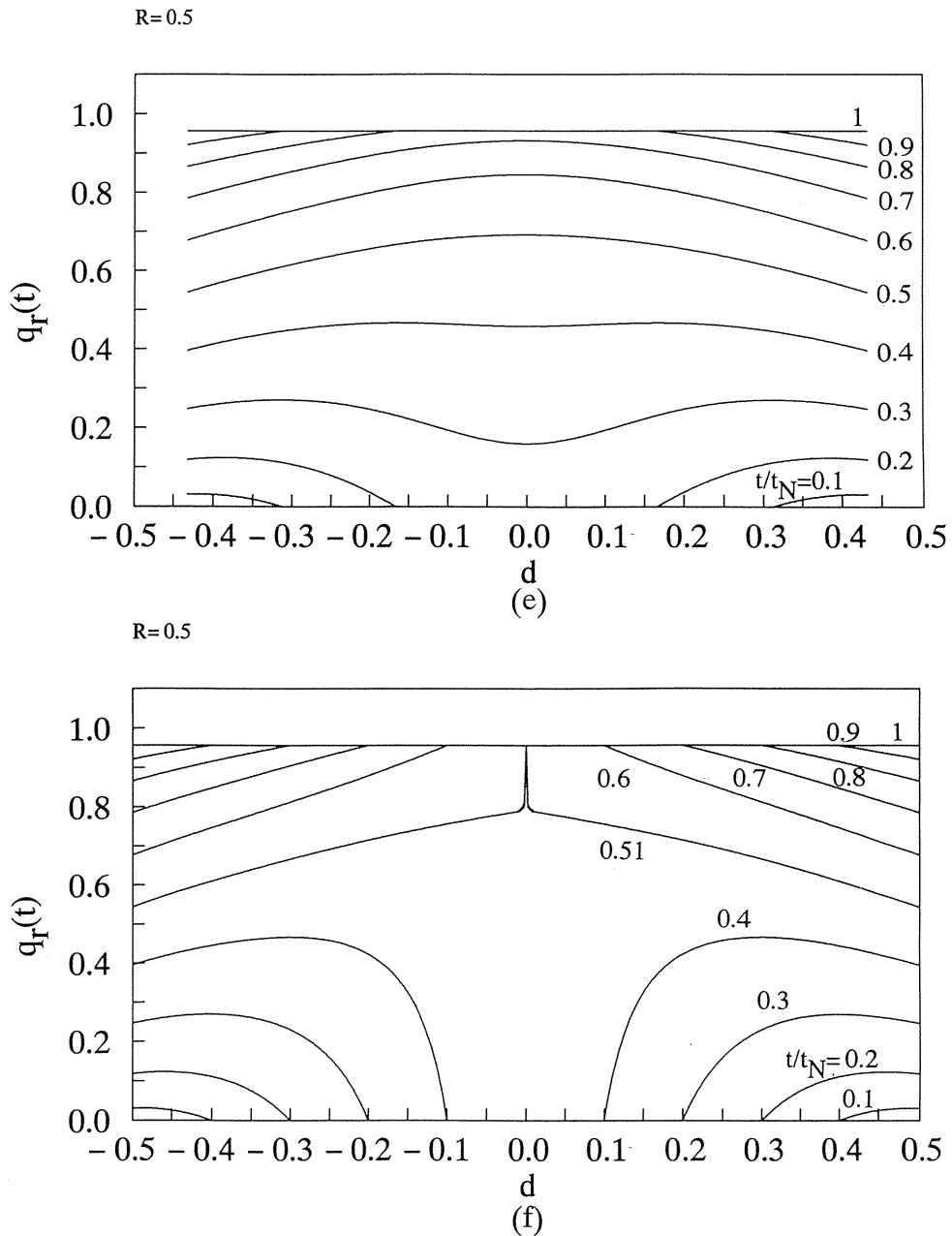


Fig. 18  $q_r(t)$  for the inward growth for various  $t$ . Category II.

For (a)–(c),  $\nu = 1$ ,  $J = 1$ ,  $R = 5$ , and (a)  $r_0 = 3.75$ , (b)  $r_0 = 2.5$  and (c)  $r_0$ . For (d)–(f),  $\nu = 1$ ,  $J = 1$ ,  $R = 0.5$ , and (d)  $r_0 = 0.375$ , (e)  $r_0 = 0.25$  and (f)  $r_0 = 0$ .

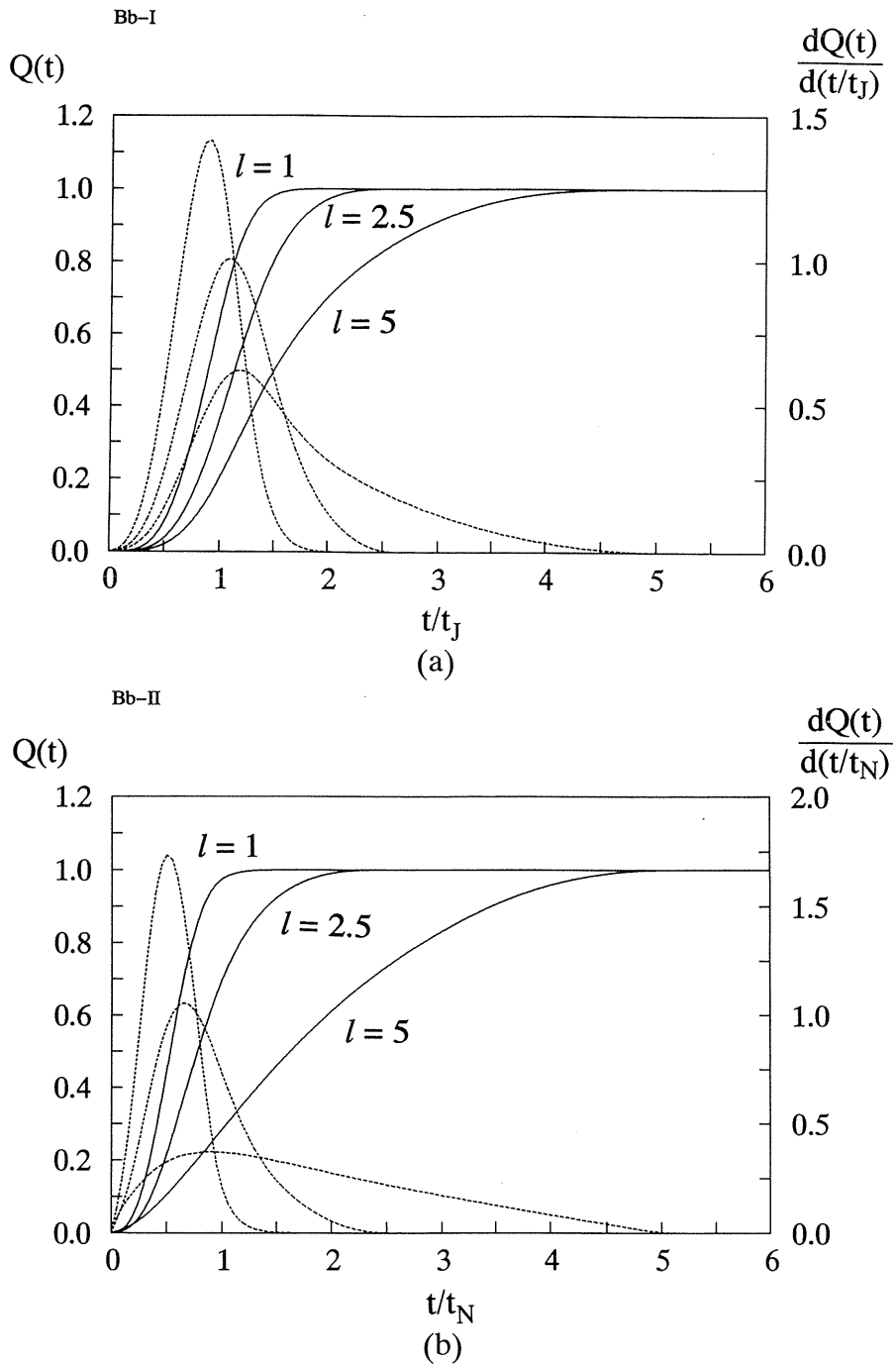


Fig. 19 The average fraction of the transformed region, for a sphere with the radius  $R$ ,  $Q(t)$  (solid lines), and its time derivative  $dQ(t)/dt$  (dashed lines). (a) Category I, and (b) category II.

### §3. Discussions

As one of applications of the Kolmogorov-Avrami model to finite systems, in this work we have studied the growth in finite volumes but without boundaries (except for surface or periphery itself). In the cases of the on-surface growth ([Aa] and [Ba] in §2), the position dependence does not appear in  $Q(t)$  in spite of the finiteness of the systems, making a contrast to the previously studied cases of finite systems with boundaries.<sup>1)</sup> Of course, in the inward growth ((Ab) and (Bb) in §2) the position dependence of  $q_A(t)$  appears as is expected.

In the cases of the on-periphery and the on-surface growth, there appear two time regimes in contrast to the inward growth cases where there appear three time regimes, as previously clarified.<sup>1)</sup> This is due to that there is no boundary in the formers.

The formulas derived in the present paper may be applied to various cases. For example, a grain in a system, which is divided into many grains and where nucleation takes place or latent nuclei exist only in grain boundaries, is just the case. Ferroelectric switching in a small area may be a case to which the present theories (Ab-I) and (Ab-II) may apply, if the switching starts at the periphery of the electroded area. In this case, the switching times  $t_s$  measured by the maximum of the switching current,  $dQ(t)/dt$ , depends upon  $R$ , a linear dimension of the area. The dependence is shown in Fig. 10.

As an example of the growth in a sphere, to which the present model is applicable, a case is conceivable where some reaction starts at the surface and proceeds inwardly.

In the present work we have treated only the cases, where the velocity,  $v$ , of advance of the boundaries is assumed to be constant. This assumption, however, is not essential. If  $v$  is a function of  $t - \tau$ , i.e., the function of the elapsed time after the nucleation, the integration appearing in the argument of the exponential function (like in (1)) should be modified accordingly. Such modification is straight-forward, according to Ref. 1.

### References

- 1) H. Orihara and Y. Ishibashi: J. Phys. Soc. Jpn. **61** (1992) 1919.
- 2) Y. Ishibashi: to be published in Proc. 4th International Symposium on Ferroelectricity, 1992, Monterey.
- 3) Y. Ishibashi and H. Orihara: J. Phys. Soc. Jpn. **61** (1992).
- 4) J.F. Scott and C.A. Araujo: Science **246** (1989) 1400.
- 5) T. Hase and T. Shiosaki: Jpn. J. Appl. Phys. **30** (1991) 2159.
- 6) B.P. Moleric, L.E. Sanchez and S.Y. Wu: Ferroelectrics **116** (1991) 65.